Supporting Information

for

FeV_3O_8/MoS_2 nanostructure heterojunctions as a highly effective electrocatalyst for hydrogen evolution

Zhi Huang[a,1], Xuejuan Tang [a,1], Junjie Zhao[a], Hua Lin[a], Ming Nie[a], Qing Li[a]*

a. Chongqing Key Laboratory for Advanced Materials and Technologies of Clean Energies, School of Materials and Energy, Southwest University, Chongqing 400715, China

*Corresponding author: E-mail: qli@swu.edu.cn

[1] *These authors contributed equally.*

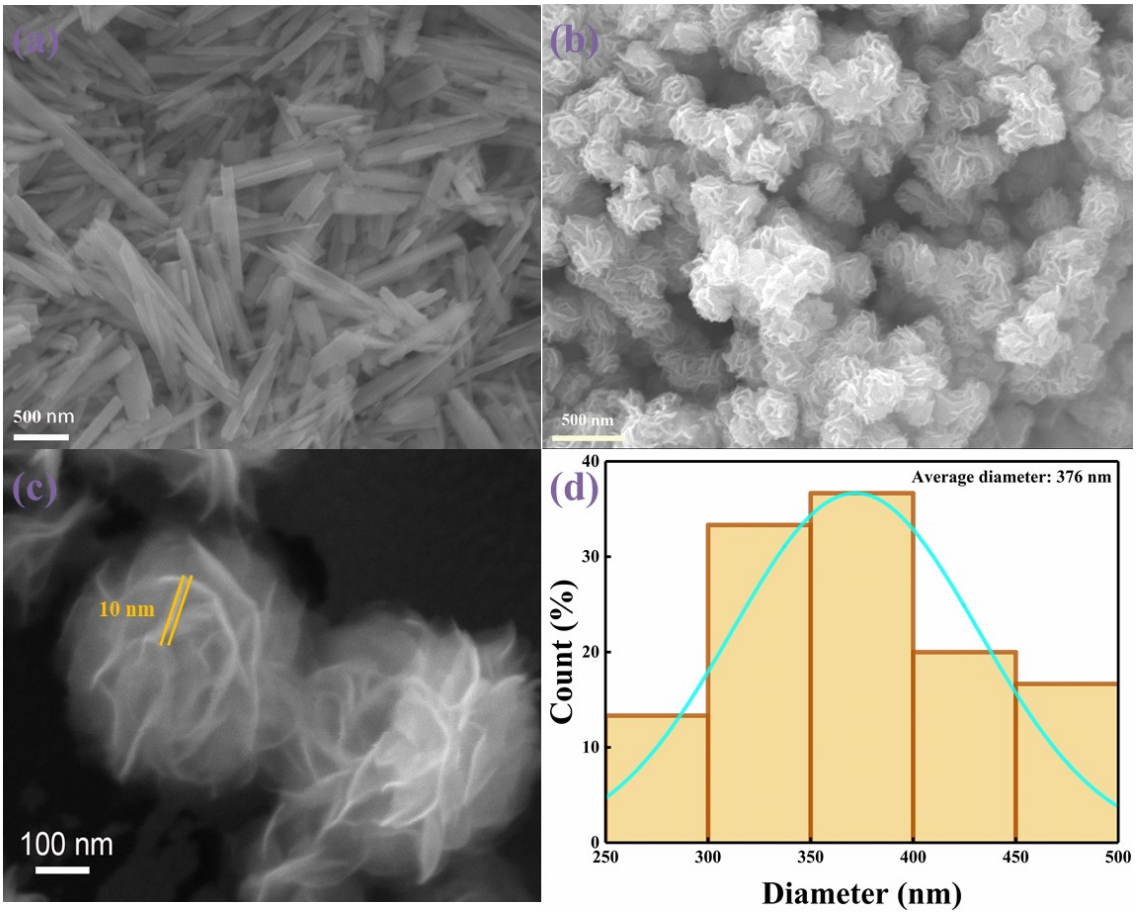

Fig. S1. (a) FESEM image of pure FeV_3O_8 nanorods, (b) Low and (c) high magnification FESEM images of GNs-MoS_2 and (d) Particle size distribution of pure MoS_2.

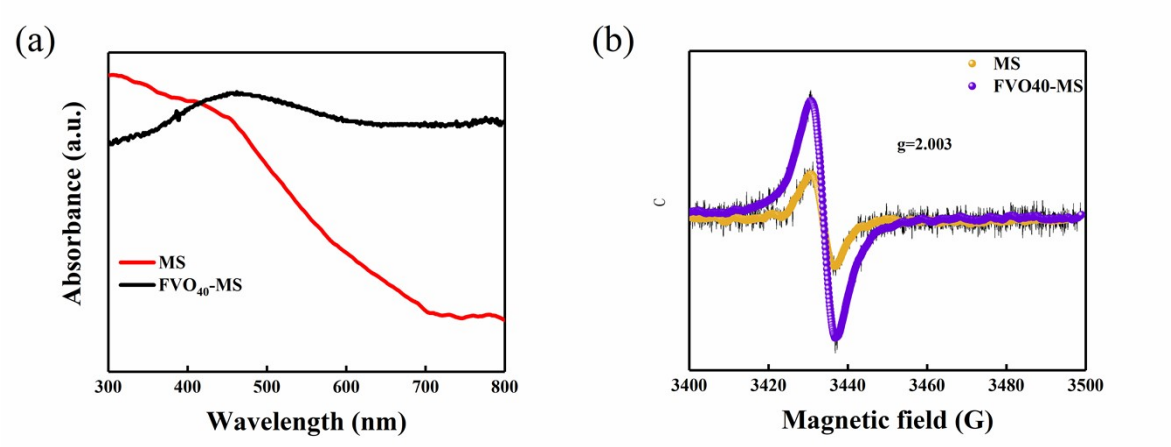

Fig. S2. (a) UV–Vis spectra of pure MoS_2 and FVO_{40}-MS, (b) EPR spectra for S vacancies of MoS_2 and FVO_{40}-MS at room-temperature.

UV-Vis and EPR analysis of the samples

UV-Vis absorption spectra and electron paramagnetic resonance (EPR) analysis were performed to gain more information for the active defects of FVO/MS heterostructure. In the UV-Vis absorption spectra (Fig. S2a), the FVO_{40}-MS shows broaden absorption peaks in the range from 400 to 800 nm compared with MS. Obviously, the absorption capacity of visible light is significantly enhanced in FVO_{40}-MS, which could be ascribed to the increased defects in FVO/MS heterojunction structure.[1, 2] Then, the room-temperature EPR was performed to further investigate the existence and the type of defects. In Fig. S2b, the FVO_{40}-MS and MS show distinct EPR signals, giving the g-value of 2.003, which could be indexed as the surface S vacancies (V_S).[3] Notably, the EPR intensity of FVO_{40}-MS is much stronger than that of pure MS, indicating that the introduction of FVO into MS brings more defects of V_S in FVO/MS heterojunction structure.[3, 4] The greatly enhanced V_S in the FVO/MS heterostructure leads to the decreasing of spontaneous non-radiative recombination from the trap states,[5-7] which resulted the enhancement of the fluorescence intensity.

References:

1. M. Dan, J. Xiang, F. Wu, S. Yu, Q. Cai, L. Ye, Y. Ye and Y. Zhou, Appl. Catal., B, 2019, 256.
2. Y. Wu, X. Chen, J. Cao, Y. Zhu, W. Yuan, Z. Hu, Z. Ao, G. W. Brudvig, F. Tian,

J. C. Yu and C. Li, Appl. Catal., B, 2022, 303.
3. M. Dan, J. Xiang, F. Wu, S. Yu, Q. Cai, L. Ye, Y. Ye and Y. Zhou, Appl. Catal., B, 2019, 256.
4. S. Jiang, N. Ji, X. Diao, H. Li, Y. Rong, Y. Lei and Z. Yu, Chemsuschem, 2021, 14, 4377-4396.
5. L. Xu, L. Zhao, Y. Wang, M. Zou, Q. Zhang and A. Cao, Nano Res, 2019, 12, 1619-1624.
6. X. Zhu, M. Du, J. Feng, H. Wang, Z. Xu, L. Wang, S. Zuo, C. Wang, Z. Wang, C. Zhang, X. Ren, S. Priya, D. Yang and S. Liu, Angew. Chem., Int. Ed., 2021, 60, 4238-4244.
7. Y. Miao, G. Sathiyan, H. Wang, Y. Tian, C. Chen, X. Ding, M. Zhai, X. Yang and M. Cheng, Chem. Eng. J, 2021, 426.

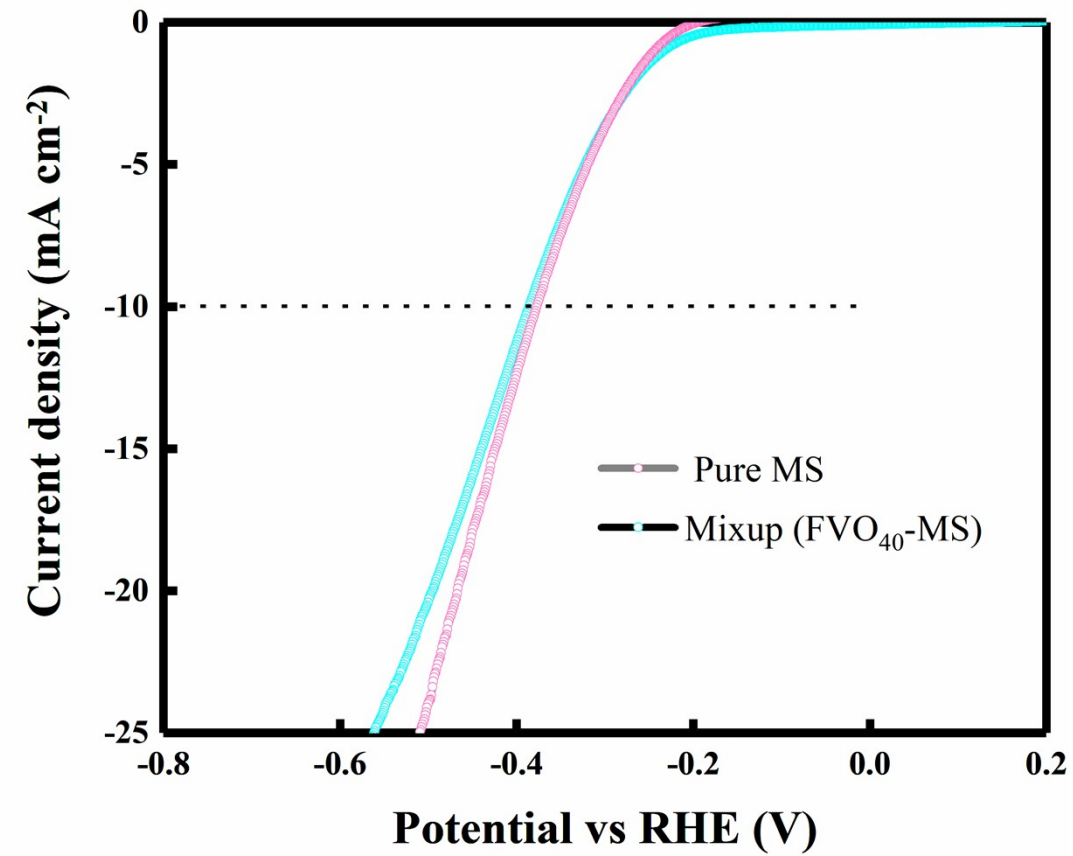

Fig. S3. LSV curve of FVO/MS mechanical mixing up in the same proportion of FVO_{40}- MS served as a contrast to pure MS.

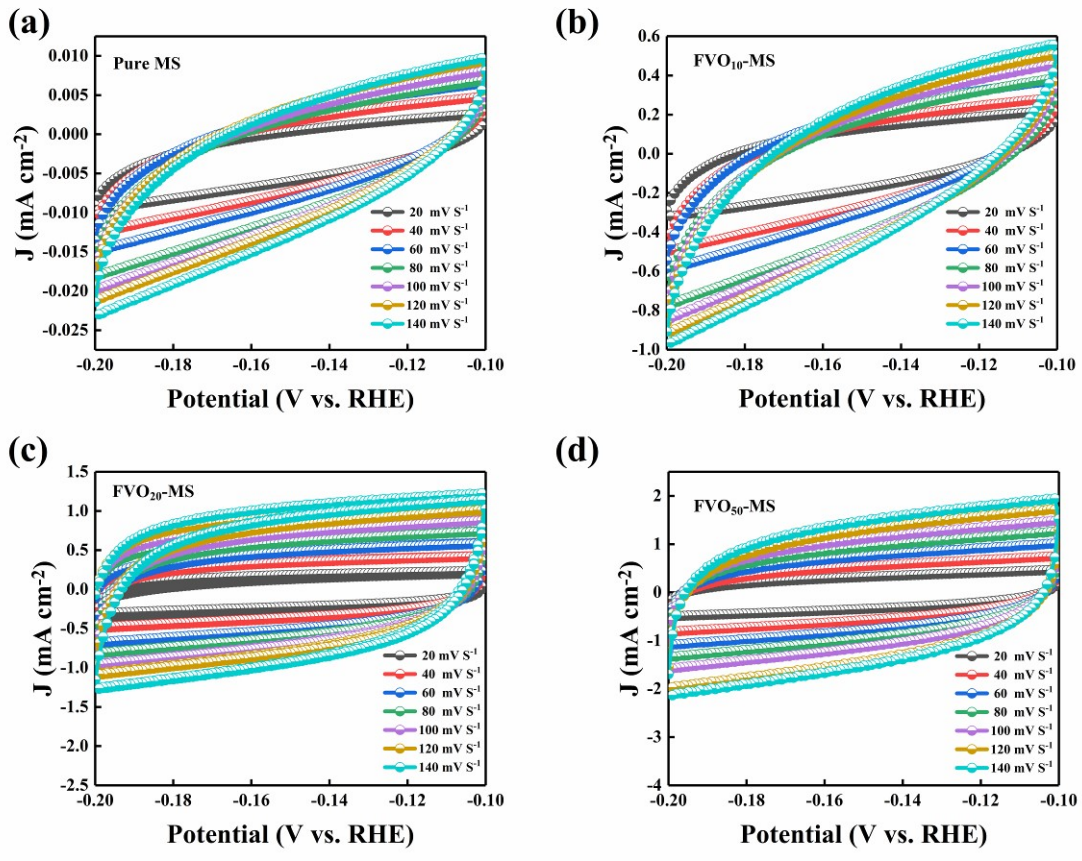

Fig. S4. The Cyclic voltammetry curves of (a) MS; (b) FVO_{10}-MS; (c) FVO_{20}-MS and (d) FVO_{50}-MS at various scan rates (20-140 mV/s) in the region of -0.1~ -0.2 V.

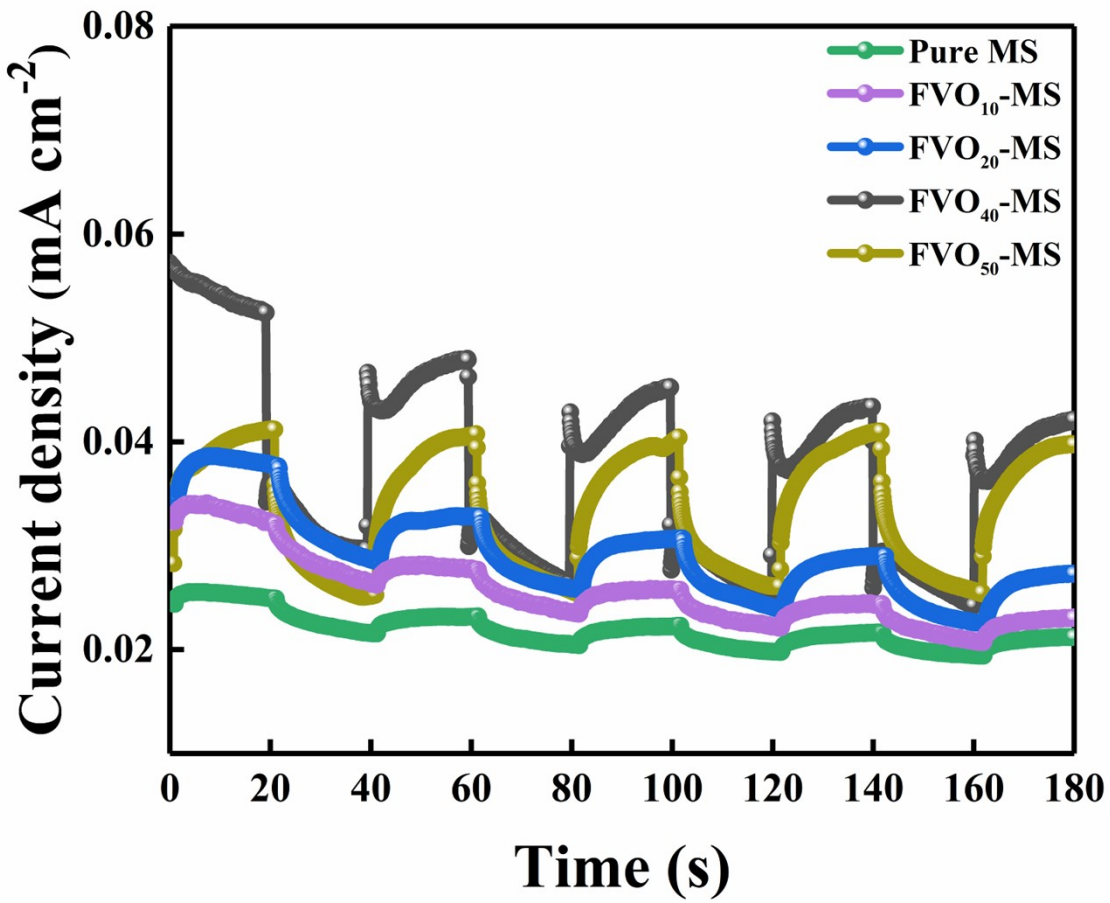

Fig. S5. (a) Transient photocurrent responses of the as-prepared samples under visible light; (b) Nitrogen adsorption–desorption isotherms of pure MoS_2 and FVO_{40}-MS.

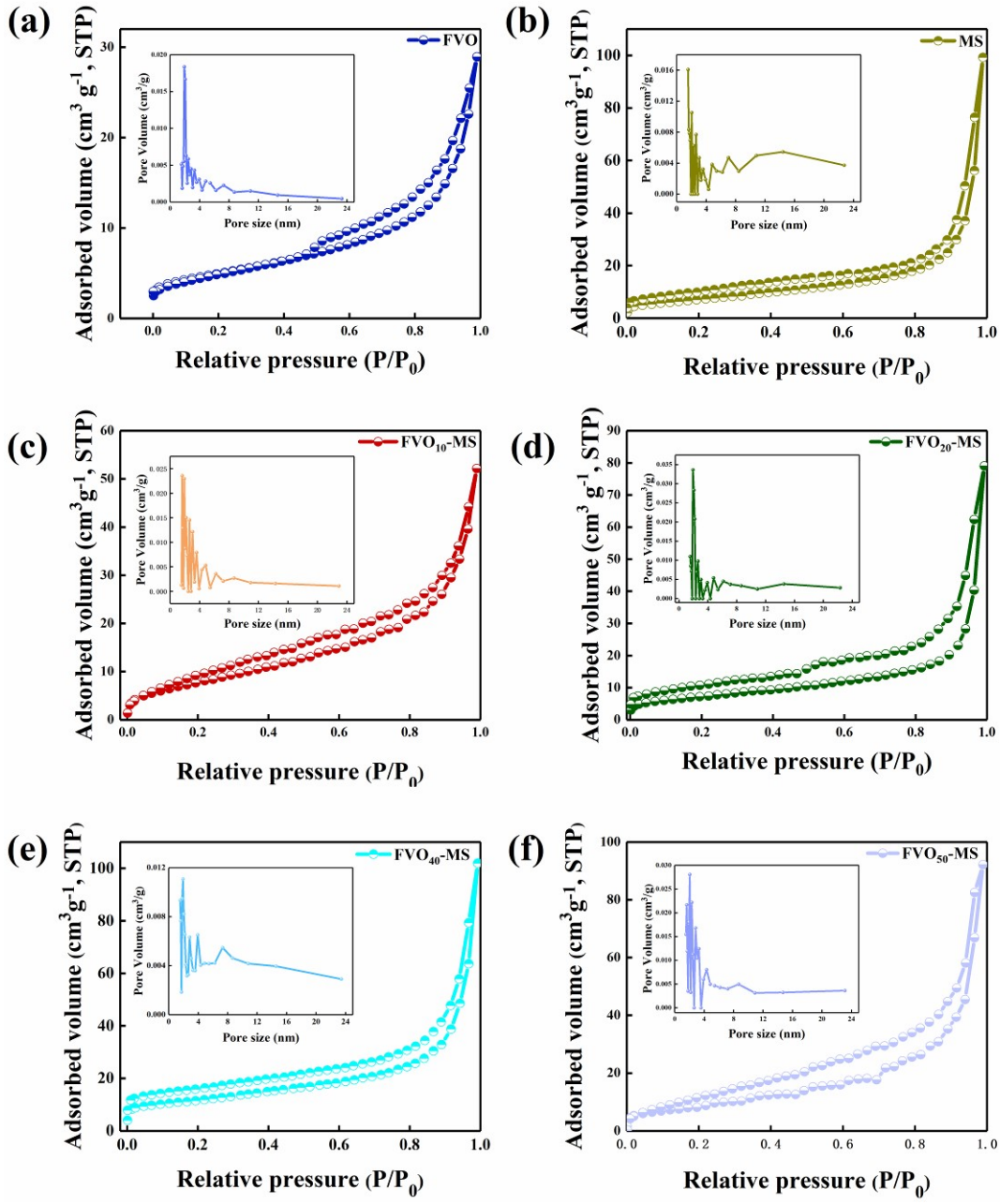

Fig. S6. Nitrogen adsorption–desorption isotherms and the corresponding pore size distribution curves of (a) FVO, (b) MS, (c) FVO_{10}-MS, (d) FVO_{20}-MS, (e) FVO_{40}-MS and (f) FVO_{50}-MS.

UV-Vis DRS and UPS analysis of the as-prepared samples

To further estimate the band gap structure of MS, FVO and FVO_{40}-MS, the UV–Vis diffuse reflectance spectrum (UV-Vis DRS) and ultraviolet photoelectron spectroscopy (UPS) analysis were carried out (Fig. S8). The band gap energy was determined based on the UV-Vis DRS absorption spectrum curve and calculated according to equation 1 (see ref.7) : $\alpha h\nu = A\ (h\nu - E_g)^{n/2}$, in which α, v, A, and Eg are the absorption coefficient, light frequency, proportionality constant, and band gap, respectively. The value of n depends on the characteristic of optical transition of the material. For FeV_3O_8 (direct semiconductor), n is 1 (see ref.9); while for MoS_2 (indirect semiconductor), n=4 (see ref.10). Bandgap curves of FeV_3O_8 and MoS_2 were collected using the Tauc plot based on the UV-Vis DRS data (Fig. S7a-7c). The value of the intersection of the tangent line with the horizontal axis represents the bandgap energy. The Eg of FeV_3O_8 and MoS_2 were 2.4 eV and 2.0 eV, respectively.

The work function (W_f) obtained from UPS study are used to investigate the behaviors of charge separation and transfer along the FVO/MS heterojunction. The calculation of W_f is based on the following equation: $W_f = h\nu - E_{onset}$ (see ref.11), where W_f was determined by subtracting the secondary cut off edge value (E_{onset}) with linear extrapolation towards the background from the He–I excitation light source (hv, 21.2 eV). From the UPS results (Fig. S7d-7f), the W_f of the FVO, MS and FVO_{40}-MS are 5.5 eV, 5.3 eV and 5.6 eV. Thus the valence band (VB) for FeV_3O_8 and MoS_2 are calculated to 2.2 eV and 1.9 eV, respectively. W_f was defined as the energy required to remove an electron at the E_f deep-seated inside the material and place it at infinity (E_{VAC}=0), which is based on the formula: $E_f = E_{VAC} - W_f$ (see ref.11). Thus, the value of E_f for FVO, MS and FVO_{40}-MS are -5.5 eV, -5.3 eV and -5.6 eV, respectively. Then, the conduction bands (CB) of FeV_3O_8 and MoS_2 are calculated via equation 2 (see ref.7): $E_{CB} = E_{VB} - E_g$, and the corresponding E_{CB} values are -0.2 eV and -0.1 eV, respectively. The detailed parameters of band structure for pure FeV_3O_8 and MoS_2 are shown in Fig. S8a. When FeV_3O_8/MoS_2 heterostructure was formed, there will be a shift of Femi levels in the semiconductor interface owing to the different W_f (see ref.8). In general, electrons transfer from a higher Fermi level to a lower one. According to the results of UPS measurement, the W_f of pure FeV_3O_8 (5.5 eV) is higher than that of MoS_2 (5.3 eV). Therefore, the band bending of MoS_2 is upward, while the band bending of FeV_3O_8 is downward (see Fig. S8b and ref.13). Based on

the relative energy band structure of FeV_3O_8 and MoS_2, the charge transfer route of FVO/MS belongs to Type-I heterojunction (see ref.14 and ref.15). The electrons in VB of FeV_3O_8 are excited to the CB under light illumination. Then, the photo-generated electrons will immediately shift to the CB of MoS_2. As lots of photo-induced electrons rapidly migrate to the active sites at the edge of MoS_2 nanosheet and participate the hydrogen evolution reaction, the HER activity of the MoS_2 was significantly enhanced.

References：

8. T. Yu, Q. Liu, Z. Zhu, W. Wu, L. Liu, J. Zhang, C. Gao and T. Yang, *Sep. Purif. Technol.*, 2021, 277, 119276.
9. L.F. Zhang, J. Zhou and C.-Y. Zhang, J. Mater. Chem. A, 2014, 2, 14903-14907.
10. S. Tongay, J. Zhou, C. Ataca, K. Lo, T. S. Matthews, J. Li, J. C. Grossman and J. Wu, Nano Lett., 2012, 12, 5576-5580.
11. W. M. Huang, W. S. Liao, Y. M. Lai and I. W. P. Chen, J. Mater. Chem. C, 2020, 8, 510-517.
12. A. Atxabal, T. Arnold, S. Parui, E. Zuccatti, M. Cinchetti, F. Casanova, F. Ortmann and L. E. Hueso, Mater. Horiz., 2019, 6, 1663-1668.
13. Y. Li, P. Zhang, D. Wan, C. Xue, J. Zhao and G. Shao, Appl. Surf. Sci., 2020, 504, 144361.
14. P. Yang, Z. Zhang, M. Sun, F. Lin, T. Cheng, J. Shi, C. Xie, Y. Shi, S. Jiang, Y. Huan, P. Liu, F. Ding, C. Xiong, D. Xie and Y. Zhang, Acs Nano, 2019, 13, 3649-3658.
15. T. Jiang, T. Xie, L. Chen, Z. Fu and D. Wang, Nanoscale, 2013, 5, 2938-2944.

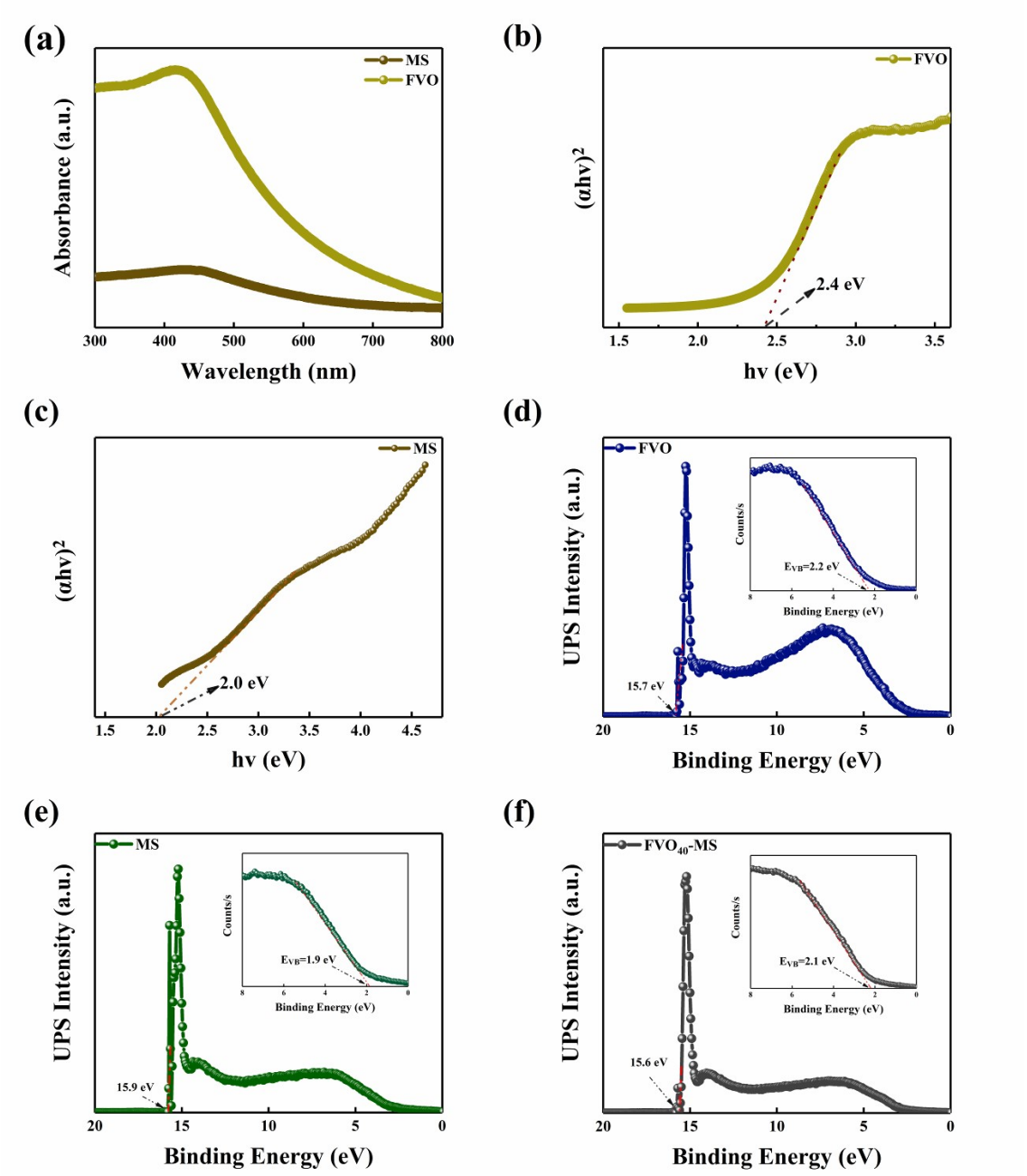

Fig. S7. (a) UV–Vis DRS spectra of MoS_2 and FeV_3O_8, Tauc plot of (b) MoS_2 and (c) FeV_3O_8, (d-f) UPS spectra and corresponding E_{CB} curves (inset) of FVO, MS and FVO_{40}-MS.

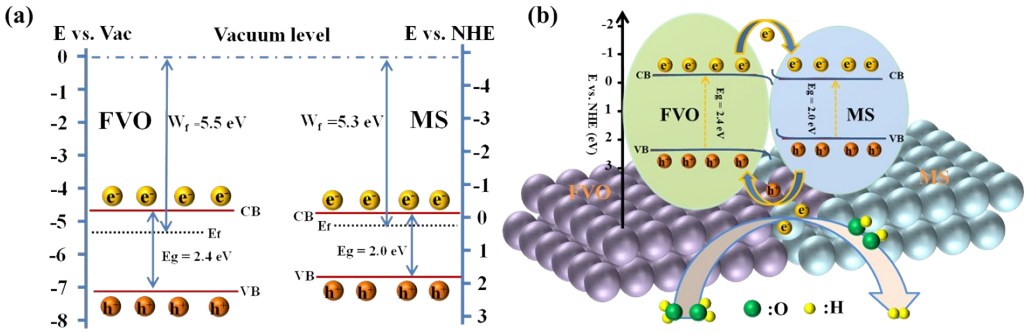

Fig. S8. (a)The band structures of FVO and MS, (b) Mechanism graph of electronic transfer in FVO/MS heterostructure.

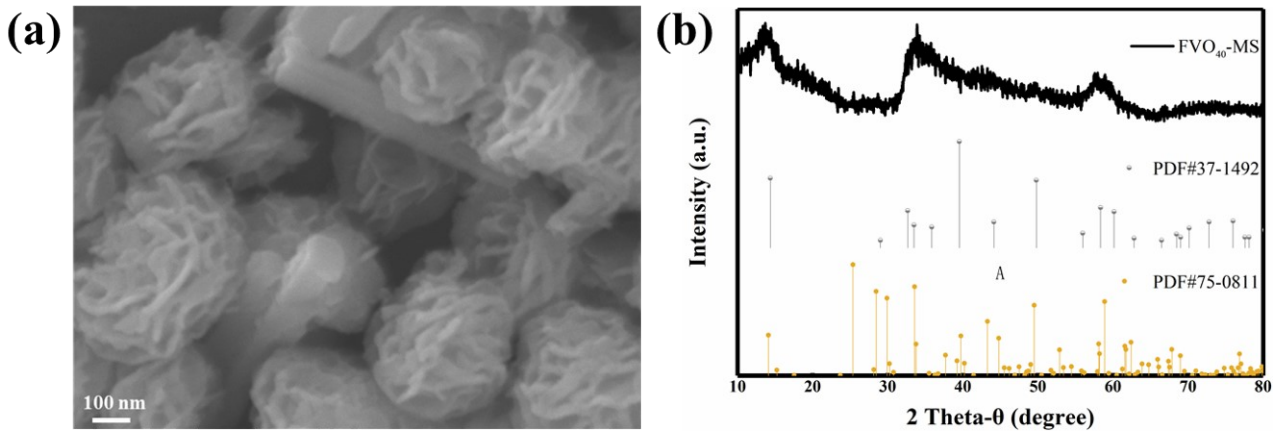

Fig. S9. (a) FESEM image and (b) XRD pattern of FVO_{40}-MS after HER tests.